Mitigation of radiation-induced fiber Bragg grating (FBG) sensor drifts in intense radiation environments based on long-short-term memory (LSTM) network

Wu, Zekun; Zaghloul, Mohamed A. S.; Carpenter, David; Li, Ming-Jun; Daw, Joshua; Mao, Zhi-Hong; Hnatovsky, Cyril; Mihailov, Stephen J.; Chen, Kevin P.

Publisher's version / Version de l'éditeur:
https://doi.org/10.1109/ACCESS.2021.3124860
IEEE Access, 9, pp. 148296-148301, 2021-11-08

IEEE Access
Multidisciplinary | Rapid Review | Open Access Journal

Received October 18, 2021, accepted October 27, 2021, date of publication November 2, 2021, date of current version November 8, 2021.

Digital Object Identifier 10.1109/ACCESS.2021.3124860

Mitigation of Radiation-Induced Fiber Bragg Grating (FBG) Sensor Drifts in Intense Radiation Environments Based on Long-Short-Term Memory (LSTM) Network

ZEKUN WU[1], MOHAMED A. S. ZAGHLOUL[1], DAVID CARPENTER[2], MING-JUN LI[3], (Fellow, IEEE), JOSHUA DAW[4], ZHI-HONG MAO[1], (Senior Member, IEEE), CYRIL HNATOVSKY[5], STEPHEN J. MIHAILOV[5], (Senior Member, IEEE), AND KEVIN P. CHEN[1]

[1]Department of Electrical and Computer Engineering, University of Pittsburgh, Pittsburgh, PA 15260, USA
[2]MIT Nuclear Reactor Laboratory, Cambridge, MA 02139, USA
[3]Corning Research and Development Corporation, Corning, NY 14831, USA
[4]Idaho National Laboratory (INL), Idaho Falls, ID 83402, USA
[5]National Research Council Canada, Ottawa, ON K1A 0R6, Canada

Corresponding author: Kevin P. Chen (pchenc@gmail.com)

This work was supported by the United States Department of Energy under Grant DE-AC07-05ID14517, Grant DE-NE0008686, and Grant DE-FE00028992.

ABSTRACT This paper reports in-pile testing results of radiation-resistant fiber Bragg grating (FBG) sensors at high temperatures, intense neutron irradiation environments, and machine learning methods for radiation-induced sensor drift mitigation and reactor anomaly identification. The in-pile testing of fiber sensors was carried out in an MIT test reactor for 180 days at a nominal operational temperature of 640°C and high neutron flux. The test results show that FBG sensors inscribed by a femtosecond laser in random airline pure silica fiber can withstand harsh environments in the reactor core but exhibit significant radiation-induced drifts. Machine learning algorithms based on long short-term memory (LSTM) networks have been used to detect reactor anomaly events and mitigate sensor drifts over a duration of up to 85 days. Through progressive supervised learning, the LSTM neural network can achieve FBG wavelength-to-temperature mapping within ±0.95°C, ±2.63°C and ±6.49°C with over 80.2%, 90%, and 95% levels of accuracy confidence, respectively. The LSTM can also identify reactor anomaly samples with an accuracy of over 94%. The results presented in this paper show that despite sensor drifts and anomaly interruptions, the LSTM-based method can effectively elucidate data harnessed by fiber sensors. Machine learning algorithms have the potential to improve situational awareness and control for a wide range of harsh environment applications, including nuclear power generation.

INDEX TERMS Fiber Bragg grating (FBG), long short-term memory (LSTM) network, radiation effects, reactor anomaly identification, supervised learning, sensor drifts mitigation, temperature measurement, wavelength-shift.

I. INTRODUCTION

Fiber optical sensors have been extensively utilized as versatile and highly multiplexable sensing devices to perform a wide array of measurements [1]. A unique feature of fiber optical sensors is their capability to perform high spatial resolution measurements using multiplexable devices such as fiber Bragg gratings (FBGs) or through various optical scattering processes [2], [3]. Well-known for their resilience to survive harsh environments, fiber optical sensors can function in environments while other sensors fail. Large datasets harnessed by fiber sensors in harsh environments

The associate editor coordinating the review of this manuscript and approving it for publication was Joewono Widjaja.

can significantly improve the safety and efficiency of various energy production processes using renewable, fossil, and nuclear fuels. However, like all other sensors intended for harsh environment applications, the performance and characteristics of fiber sensors could be influenced by the environment and incur significant drifts [4]–[7].

The deployment of fiber sensors in nuclear reactor cores to perform continuous and high spatial resolution measurements is of great interest to both civilian and military operators of nuclear energy systems. One of the most comprehensive studies of FBG sensors in harsh nuclear core environments was conducted by Fernandez and Gusarov *et al.*, who reported the use of FBGs endured gamma radiation doses up to 160MGy and neutron fluence up to 1.47×10^{17} fast neutrons per square centimeter for temperature monitoring with 3°C accuracy [7]–[10]. In 2016, Remy *et al.* reported the radiation-induced compaction (RIC) effect on FBG sensors exposed to 2.83×10^{19} fast neutrons per square centimeter with a 4°C accuracy in temperature [5]. In 2017, a number of in-pile tests were performed at the MIT test reactor (MITR) to evaluate the radiation resilience of fiber Bragg grating (FBG) sensors exposed to extremely high neutron flux ($>2 \times 10^{14}$ fast neutrons per second per square centimeter) at a nominal operational temperature of 640°C for an entire testing period of 180 days [2]. These encouraging results suggest that fiber sensors have the potential to perform high spatial resolution monitoring to improve the safety and operational efficiency of nuclear energy systems.

However, the test results show that continuous neutron irradiation exerted on FBG sensors produces drifts of fiber sensor characteristics with complex drift patterns. The overall trend of the FBG wavelength drift is approximately linear to the accumulated neutron flux, but the drift rate varies over different testing periods [2]. The continuous evolution of sensor characteristics and interruptions by simulated anomalies poses significant challenges in delineating the sensor response.

In this paper, we report a machine learning approach based on a long short-term memory (LSTM) neural network [18] to mitigate sensor drifts induced by harsh neutron and gamma irradiation and identify reactor anomaly events. LSTM is a special type of Recurrent Neural Network (RNN), which is commonly used in processing sequence data with temporal dependencies. Compared to RNN, LSTM has the advantage of handling long-term information based on the gate mechanism [19]–[21]. Modeling the long-term radiation-induced effects, including fiber compaction, can be a challenge, but LSTM can directly model the drifting data of the Bragg wavelength and learn the hidden dependencies over long testing periods. The radiation resistance of our fiber sensor makes it possible for reliable long-term learning over the entire testing period. The results presented in this paper show that the continuous data harness and training of the LSTM neural network can effectively mitigate the adverse effects of sensor drifts, leading to accurate temperature measurements and anomaly event identification.

II. EXPERIMENTS AND DEFINITIONS

Two optical fibers, pure-silica random airline (RAL) fibers and F-doped cladding single-mode fibers, were considered based on previous literature studies and the cost of fibers for potential large-scale deployment [2]. When exposed to accumulated gamma dose of 1 MGy, F-doped single-mode fibers exhibited lower radiation-induced attenuation (RIA), but larger temperature measurement error (−2.3°C) compared to pure silica core (PSC) fibers (−0.7°C) [4]. Pure silica core (PSC) fibers, which exhibit radiation-induced loss on the order of a few dB per kilometer in the infrared, are known to be one of the most radiation-resistant fibers in terms of low RIA [14]. With identical thermal expansion coefficients and similar responses under neutron or gamma radiation in both the fiber core and cladding regions, the pure-silica RAL fiber has conceivable radiation resistance, and it can also be manufactured at a much lower cost [15] compared to other pure-silica fibers such as photonic crystal fibers [11]. In this case, we selected pure silica RAL fibers.

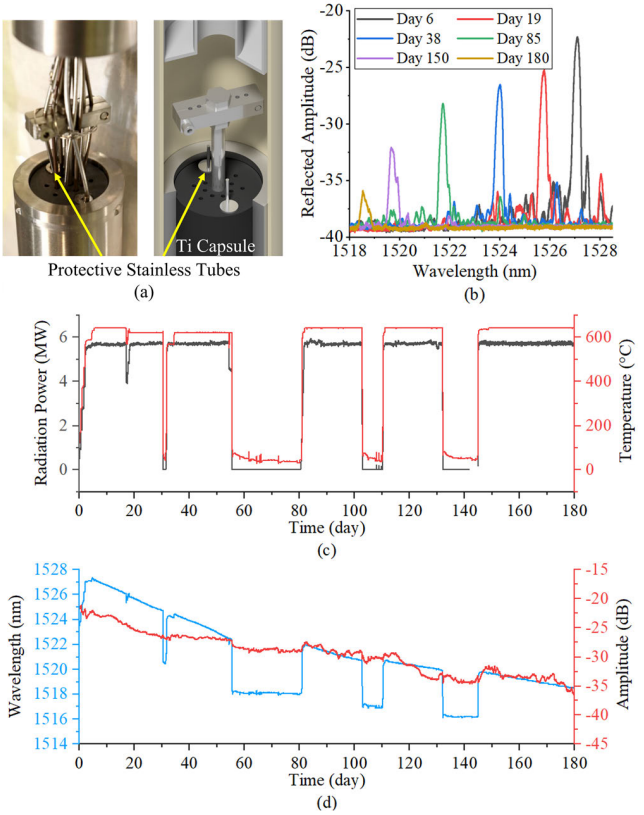

FIGURE 1. (a) Stainless-steel tubes with fiber sensor inside, inserted in Ti capsule. (b) Typical FBG spectra with different accumulated radiation effects. (c) Reactor power and temperature over 180 days. (d) FBG peak wavelength and corresponding amplitude over 180 days.

The pure-silica RAL fiber used in this study was nano-engineered using the outside vapor deposition (OVD) process [12], [13]. The FBG sensor was inscribed by a femtosecond laser through a phase-mask approach in a pure-silica random airline fiber. Details of the random airline fiber and FBG fabrication procedure can be found in [2].

Fig. 1 provides a general description of the experiment. The fiber was inserted into a stainless tube and lowered to the reactor core, as shown in Fig. 1a. The average fast neutron flux of the reactor where the fiber sensor was located was approximately 2.1×10^{14} fast neutrons per second per square centimeter. The fast neutrons are neutrons with an average kinetic energy of >0.1 MeV. The reflection spectra of the FBG were interrogated using a tunable laser (TUNICS T100S-HP) from 1510 nm to 1580 nm and acquired every 20 s continuously with a wavelength resolution of 2 pm [2]. This yield approximately 7.8×10^5 frames of spectra over 180 days. The temperature of the Ti holder in the reactor core was monitored using four thermocouples [2]. The FBG response with accumulated fluences over different testing periods is shown in Fig. 1b. It is clear that both the FBG peak wavelength and the reflected amplitude underwent significant drift.

Fig. 1c and d show the reactor power profile, temperature measured by thermocouples, FBG peak wavelength, and corresponding amplitude over 180 days. The reactor was maintained at 625°C-645°C during normal operation at approximately 5.7 MW, while simulated anomaly events were instigated, which led to sharp fluctuations in the reactor power and temperature, as shown in Fig. 1c. Four reactor states are defined to identify reactor events: Normal-Operation (NO), Anomaly Rising (AR), Anomaly Falling (AF), and Anomaly-Duration (AD).

The NO state is defined when the reactor power remains constant at approximately 5.7 MW with a temperature around 625°C-645°C. Significant drifts of the FBG peak wavelength induced by harsh neutron and gamma irradiation can be observed in Fig. 1d (day 40-50 for example).

Anomaly-Rising (AR) and Anomaly Falling (AF) states are defined when simulated anomaly events lead to sharp fluctuations in neutron power and temperature (day 55 and day 81, for example). For quantification, we chose 20 °C as an empirical threshold, given that the measured temperature varied between 625°C-645°C during normal operations. Periods between ARs or AFs are defined as Anomaly-Duration (AD). Thus, we have the following definitions:

$$s = \begin{cases} NO & 625°\text{C} \le T \le 645°\text{C} \; and \; |\Delta T| \le 20°\text{C} \\ AF & \Delta T < -20°\text{C} \\ AR & \Delta T > 20°\text{C} \\ AD & otherwise, \end{cases} \tag{1}$$

where ΔT is the temperature variation within a short period of time Δt, which will be discussed in the next section.

III. DRIFT MITIGATION SYSTEM DESIGN

Temperature and cumulative radiation are two key factors that influence FBG wavelength variations, as shown in Fig. 1c. To distinguish between temperature and radiation effects, the following relationship is defined: In a period of time $\boldsymbol{\Delta t}$, the Bragg wavelength shift (BWS) $\boldsymbol{\Delta\lambda_B}$, owing to variations in temperature $\boldsymbol{\Delta T}$ and cumulative radiation effect $\boldsymbol{C_{Rt}\Delta t}$, is given by

$$\frac{\Delta\lambda_B}{\lambda_B} = C_T \Delta T + C_{Rt} \Delta t, \tag{2}$$

where C_T is the coefficient of temperature variation and C_{Rt} is the coefficient of radiation-induced effects over a period of time. The factor Δt is defined as the period of time from an arbitrary past time t_0 to the current time t ($t_0 < t$) because we can only use samples from the past in real-world applications, and ΔT is defined as the temperature variation from t_0 to t.

Our task was to map from Bragg wavelength to the current temperature, distinguishing radiation-induced BWS. The testing periods under different reactor states provide good opportunities to distinguish $\boldsymbol{C_T\Delta T}$ and $\boldsymbol{C_{Rt}\Delta t}$. The temperature variations are nearly 0 in a single "NO" testing period, so if $\boldsymbol{\Delta t}$ is large enough for accumulation of radiation-induced effects, we can safely set $\boldsymbol{C_T\Delta T}$ to 0. As for "AF" or "AR" periods, the temperature and wavelength vary a lot within a short period of time, so if $\boldsymbol{\Delta t}$ is small enough to satisfy $|\boldsymbol{C_{Rt}\Delta t}| \ll |\boldsymbol{C_T\Delta T}|$, we can also set $\boldsymbol{C_{Rt}\Delta t}$ to 0 and estimate the other coefficient.

However, the continuous evolution of sensor characteristics will finally result in the evolution of these two coefficients over the entire testing period, and the coefficients calculated from one testing period may not be reliable in the next period. Therefore, we prefer a machine learning tool to build a more flexible model. It is worth noting that the machine learning tool also tends to distinguish $\boldsymbol{C_T\Delta T}$ from $\boldsymbol{C_{Rt}\Delta t}$ to perform accurate mapping from BWS to temperature; therefore, an appropriate $\boldsymbol{\Delta t}$ will also improve the accuracy of the model.

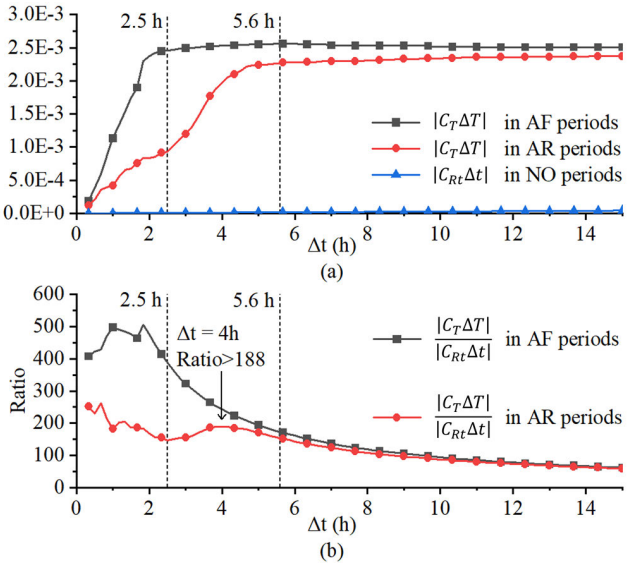

FIGURE 2. (a) Values of $|C_T\Delta T|$ and $|C_{Rt}\Delta t|$ versus Δt and (b) ratio of $|C_T\Delta T|$ to $|C_{Rt}\Delta t|$ versus Δt based on the samples of day 10 to 95.

Based on the samples from day 10 to 95, the values of $|\boldsymbol{C_{Rt}\Delta t}|$ and $|\boldsymbol{C_T\Delta T}|$ versus $\boldsymbol{\Delta t}$ are shown in Fig. 2a. The values $|\boldsymbol{C_{Rt}\Delta t}|$ are averaged from all the "NO" testing periods

from day 10 to 95, and values $|\boldsymbol{C_T \Delta T}|$ are averaged from all the "AF" or "AR" periods from day 10 to 95 based on different $\boldsymbol{\Delta t}$. When $\boldsymbol{\Delta t}$ is approximately 2.5h or 5.6h, the temperature stops falling or rising, respectively. Fig. 2b shows that from 2.5h to 5.6h, the largest ratio for AR periods appears at approximately 4h. We also hope that the ratios for periods AR and AF are close to each other for less learning bias. Thus, $\boldsymbol{\Delta t}$ was selected to 4h.

The LSTM network we developed consists of a two-channel input layer, an LSTM layer with 200 hidden units, a fully connected layer, and a regression output layer. Based on (2), we set the Bragg wavelength and wavelength shift $[\boldsymbol{\lambda_B \Delta\lambda_B}]$ as two-channel features to the input layer. The LSTM layer contains blocks corresponding to every time step, passing information from all previous samples regardless of the length of the sequence, and the gate mechanism controls the addition or removal of information at each time step. This is how LSTM learns long-term dependencies. The number of hidden units determines the amount of information that LSTM remembers over time steps; thus, we set 200 as an empirical number to prevent overfitting. The fully connected layer connects all the neurons and compiles data from previous LSTM layers, preparing for the final output. Because the wavelength-to-temperature mapping is a sequence-to-sequence regression task, the fully connected layer is followed by a regression output layer, which computes the half-mean-squared-error loss of the predicted temperature for each time step. We set the training target as $\boldsymbol{T}$ rather than $\boldsymbol{\Delta T}$ to mitigate the error accumulated by adding the predicted $\boldsymbol{\Delta T}$ together. Based on (1), the reactor state series $\boldsymbol{s}$ is determined by the predicted $[\boldsymbol{T\,\Delta T}]$.

The network was trained on the first 95 days for 100 epochs and tested on the remaining 85 days. Fig. 3 shows the drift mitigation and anomaly identification diagram. Data pre-processing was carried out to find the Bragg wavelength ($\boldsymbol{\lambda_B}$) and wavelength shift ($\boldsymbol{\Delta\lambda_B}$) in a specific time period ($\boldsymbol{\Delta t}$ as mentioned above).

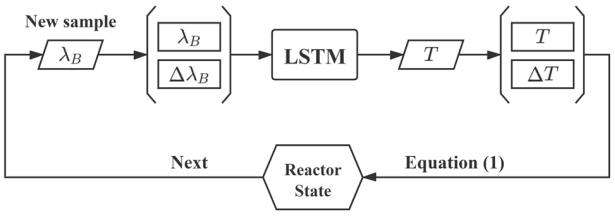

FIGURE 3. Drift mitigation and anomaly identification diagram.

If the reactor state is "AD," the reactor operates at a lower power, and the radiation level and temperature are steady in the lower range. Thus, neither temperature nor radiation-related terms were sufficiently large to estimate the coefficients. As this study focuses on drift mitigation (NO state) and anomaly identification (AF and AR states), we omitted AD periods.

IV. RESULTS AND DISCUSSION

As mentioned in Section 3, both temperature and radiation effects, as two key factors, contribute to the wavelength shift of the FBG temperature sensor. We compared the predicted and measured temperatures to evaluate the drift-mitigation results, as shown in Fig. 4a. The AD periods were omitted, as explained in Section 3. Day 1-95 and 96-180 are the training and testing periods, respectively. Once trained by data from day 1-95, the network has never been updated over the entire testing period. Fig. 4b shows the prediction accuracies for various error tolerances. Accuracy confidence levels over 80.2%, 90%, and 95% were achieved within error tolerances of ±0.95°C, ±2.63°C and ±6.49°C, respectively.

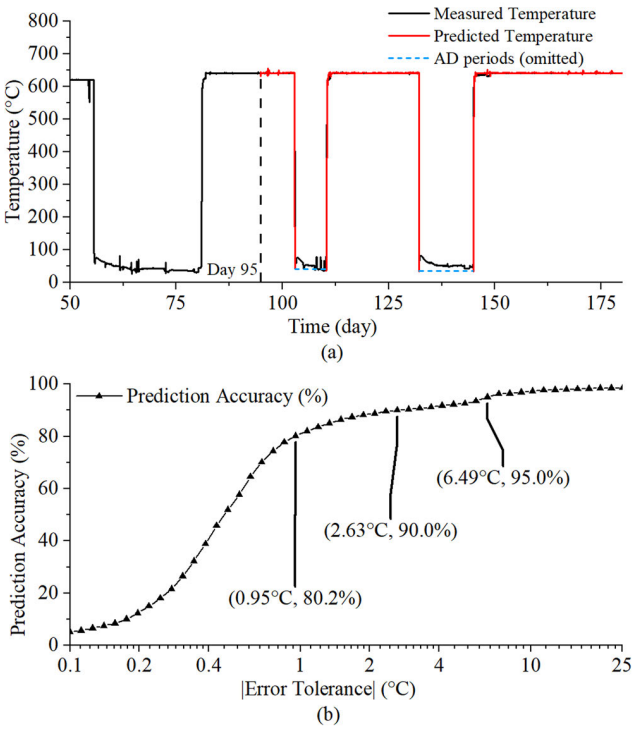

FIGURE 4. (a) Temperature predicted by LSTM from day 95 to day 180. (b) Prediction accuracies over different error tolerances from ±0.1°C to ±25°C.

It is worth noting that we did not update our LSTM network using new samples after the training period because we hope to see if our network can be flexible to the continuous evolution of sensor characteristics. It can be observed from Fig. 1d that the wavelength drifting rates in the training period (day 1-95) are different from the testing period and continuously change over such a long-term testing. The results in Fig. 4a show that our LSTM network can still achieve the mapping from wavelength to temperature even after day 150. This proves the potential of the machine learning tool to be flexible for the complicated evolution of sensor characteristics.

Table 1 lists the anomaly identification accuracies based on the predicted temperatures. Our LSTM network achieved 100% anomaly event identification and over 96.6% and

TABLE 1. Anomaly detection accuracy.

Anomaly	Events Identified	Samples Detected	False alarm
Anomaly-Falling (AF)	100%	96.6%	0.85%
Anomaly-Rising (AR)	100%	94.3%	2.12%

94.3% detection accuracy for samples under AF and AR states, respectively. Most of the missed or false alarm samples are around "AF" or "AR" testing periods. About 0.85% and 2.12% samples were incorrectly detected as "AF" or "AR", respectively.

Because anomaly detection is based on the temperature predicted by the LSTM network, as shown in Fig. 3, the detection accuracy depends on the mapping accuracy from wavelength to temperature.

To improve the performance of the LSTM network, updating the network parameters with new samples is still a good option, especially for real-time applications. The updating process can be repeated after a specific period of time to collect sufficient new samples. Although other temperature sensors such as thermocouples are required for reference, FBGs still have many advantages such as less response time, high sensitivity, less temperature leakage through cabling, and the ability to monitor the local temperature [16], [17].

Another factor, $\boldsymbol{\Delta t}$ also plays an important role because it controls the length of the time period to calculate wavelength and temperature variation. The selection of $\boldsymbol{\Delta t}$ is based on training samples, as described in Section 3, but in real-time application, the proper value of $\boldsymbol{\Delta t}$ may vary over time. A possible solution is to update the network by different $\boldsymbol{\Delta t}$ values and estimate a proper range after a specific time period. This can be included in the updating process described above. Another solution is to train an end-to-end model to directly map the Bragg wavelength or amplitude to temperature, skipping the calculation of the relative wavelength shift.

V. CONCLUSION

This paper demonstrates the resilience of fiber sensors in the extremely harsh environment of an operating nuclear reactor core and the effectiveness of the machine learning approach. This application of an LSTM neural network shows that radiation-induced sensor drifts and overall FBG peak wavelength degradation can be effectively mitigated. The machine learning approach shows great potential for improving the measurement accuracy for anomaly identification and overall reactor performance monitoring.

REFERENCES

[1] S. Yin, P. B. Ruffin, and T. S. Francis, Eds., *Fiber Optic Sensors*. Boca Raton, FL, USA: CRC Press, 2017.

[2] M. A. Zaghloul, M. Wang, S. Huang, C. Hnatovsky, D. Grobnic, S. Mihailov, M. J. Li, D. Carpenter, L. W. Hu, J. Daw, and G. Laffont, "Radiation resistant fiber Bragg grating in random air-line fibers for sensing applications in nuclear reactor cores," *Opt. Exp.*, vol. 26, no. 9, pp. 11775–11786, 2018.

[3] O. Frazão, C. Correia, J. L. Santos, and J. M. Baptista, "Raman fibre Bragg-grating laser sensor with cooperative Rayleigh scattering for strain–temperature measurement," *Meas. Sci. Technol.*, vol. 20, no. 4, Apr. 2009, Art. no. 045203.

[4] A. Morana, S. Girard, E. Marin, C. Marcandella, S. Rizzolo, J. Périsse, J. R. Macé, A. Taouri, A. Boukenter, M. Cannas, and Y. Ouerdane, "Radiation vulnerability of fiber Bragg gratings in harsh environments," *J. Lightw. Technol.*, vol. 33, no. 12, pp. 2646–2651, Jun. 15, 2015.

[5] L. Remy, G. Cheymol, A. Gusarov, A. Morana, E. Marin, and S. Girard, "Compaction in optical fibres and fibre Bragg gratings under nuclear reactor high neutron and gamma fluence," *IEEE Trans. Nucl. Sci.*, vol. 63, no. 4, pp. 2317–2322, Aug. 2016.

[6] S. J. Mihailov, "Fiber Bragg grating sensors for harsh environments," *Sensors*, vol. 12, no. 2, pp. 1898–1918, 2012.

[7] A. Gusarov and S. K. Hoeffgen, "Radiation effects on fiber gratings," *IEEE Trans. Nucl. Sci.*, vol. 60, no. 3, pp. 2037–2053, Jun. 2013.

[8] A. Gusarov, A. F. Fernandez, S. Vasiliev, O. Medvedkov, M. Blondel, and F. Berghmans, "Effect of gamma-neutron nuclear reactor radiation on the properties of Bragg gratings written in photosensitive Ge-doped optical fiber," *Nucl. Instrum. Methods Phys. Res. B, Beam Interact. Mater. At.*, vol. 187, pp. 79–86, Jan. 2002.

[9] A. F. Fernandez, A. I. Gusarov, B. Brichard, S. Bodart, K. Lammens, F. Berghmans, M. C. Decreton, P. Megret, M. Blondel, and A. Delchambre, "Temperature monitoring of nuclear reactor cores with multiplexed fiber Bragg grating sensors," *Opt. Eng.*, vol. 41, no. 6, pp. 1246–1254, Nov. 2002.

[10] A. Gusarov, "Long-term exposure of fiber Bragg gratings in the BR1 low-flux nuclear reactor," *IEEE Trans. Nucl. Sci.*, vol. 57, no. 4, pp. 2044–2048, Aug. 2010.

[11] H. Henschel, J. Kuhnhenn, and U. Weinand, "High radiation hardness of a hollow core photonic bandgap fiber," in *Proc. 8th Eur. Conf. Radiat. Effects Compon. Syst.*, Sep. 2005, pp. LN4-1–LN4-4.

[12] D. C. Bookbinder, R. M. Fiacco, M. J. Li, M. T. Murtagh, and P. Tandon, "Microstructured optical fibers and methods," U.S. Patent 7 450 806, Nov. 11, 2008.

[13] M.-J. Li, P. Tandon, D. Bookbinder, D. Nolan, S. Bickham, M. McDermott, R. Desorcie, J. Englebert, S. Logunov, V. Kozlov, and J. West, "Nano-engineered optical fibers and applications," in *Proc. Opt. Fiber Commun. Conf.*, Mar. 2010, pp. 1–3.

[14] A. Cusano, A. Cutolo, and J. Albert, Eds., "Fiber Bragg grating sensors in nuclear environments," in *Fiber Bragg Grating Sensors: Recent Advancements, Industrial Applications and Market Exploitation*. Sharjah, United Arab Emirates: Bentham Science, 2011, ch. 12, Sec. 4, pp. 226–227.

[15] C. Roberts and R. Ellis, "Fiber selection and standards guide for premises networks," *Corning White Paper*, vol. 8, no. 8, pp. 2–5, 2013.

[16] S. Abad, "Applications of FBG sensors on telecom satellites," *Proc. SPIE*, vol. 10565, Nov. 2017, Art. no. 1056517.

[17] F. Wu, J. Zhao, B. Liu, and Y. Zhang, "Study on local temperature characteristics of fiber Bragg gratings," *Optoelectron. Lett.*, vol. 6, no. 2, pp. 98–102, Mar. 2010.

[18] S. Hochreiter and J. Schmidhuber, "Long short-term memory," *Neural Comput.*, vol. 9, no. 8, pp. 1735–1780, 1997.

[19] F. A. Gers, J. Schmidhuber, and F. Cummins, "Learning to forget: Continual prediction with LSTM," *Neural Comput.*, vol. 12, no. 10, pp. 2451–2471, 2000.

[20] R. Jozefowicz, W. Zaremba, and I. Sutskever, "An empirical exploration of recurrent network architectures," in *Proc. 32nd Int. Conf. Mach. Learn. (ICML)*, Lille, France, 2015, pp. 2342–2350.

[21] M. A. S. Zaghloul, A. M. Hassan, D. Carpenter, P. Calderoni, J. Daw, and K. P. Chen, "Optical sensor behavior prediction using LSTM neural network," in *Proc. IEEE Photon. Conf. (IPC)*, Sep. 2019, pp. 1–2.

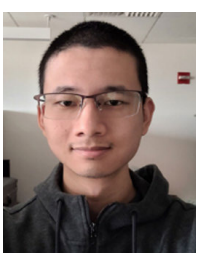

ZEKUN WU was born in Qianxi, Tangshan, Hebei, China, in 1996. He received the B.S. degree in opto-electronic engineering from the Beijing Institute of Technology, China, in 2018, and the M.S. degree in electrical and computer engineering from the University of Pittsburgh, PA, USA, in 2019, where he is currently pursuing the Ph.D. degree with the School of Electrical and Computer Engineering.

His current research interests include optical sensing and imaging systems.

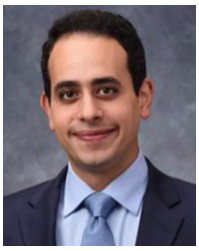

MOHAMED A. S. ZAGHLOUL received the B.S. degree in electronics and electrical communications engineering and the M.S. degree in engineering physics from the Faculty of Engineering, Cairo University, Giza City, Giza, Egypt, in 2009 and 2012, respectively, and the Ph.D. degree from the Department of Electrical and Computer Engineering, University of Pittsburgh, Pittsburgh, PA, USA, in 2019.

He is currently an Assistant Professor with the University of Pittsburgh. His research interests include optics and specializes in developing optical fiber-based sensors for monitoring harsh environments.

DAVID CARPENTER received the B.S. and M.S. degrees in nuclear science and engineering from the Massachusetts Institute of Technology, Cambridge, MA, USA, in 2006, and the Ph.D. degree from the Massachusetts Institute of Technology, in 2010.

He is currently with the Nuclear Reactor Laboratory, Massachusetts Institute of Technology. His research interests include the development of innovative facilities and data acquisition for in-core irradiation testing of fuel and materials, light water reactor fuel and cladding development, including modeling and irradiation studies, and material characterization with regard to radiation damage and corrosion.

MING-JUN LI (Fellow, IEEE) received the B.S. degree in applied physics from the Beijing Institute of Technology, Beijing, China, in 1983, the M.S. degree in optics and signal processing from the University of Franche-Comte, Besancon, France, in 1985, and the Ph.D. degree in physics from the University of Nice, Nice, France, in 1988.

He joined Corning Incorporated, in 1991, where he is currently a Corporate Fellow. He has contributed to many fiber products, including bend insensitive fiber for FTTH, large effective area fiber, ultra-low PMD fiber and ultra-low loss fiber for high data rate transmission, low SBS fiber for analog transmission, high bandwidth MMF for data centers, various specialty fibers for connectors, fiber lasers, sensors and endoscopes, multicore fibers and few mode fibers for space division multiplexing, and new glass waveguide devices for optical interconnect and sensing applications. He holds 250 U.S. patents and has published six book chapters and over 320 papers in journals and conferences.

Dr. Li is a member of the U.S. National Academy of Engineering and a fellow of the Optica. He was elected into the National Inventors Hall of Fame for ClearCurve bend-insensitive optical fiber, in 2020. He received the 1988 French National Prize on Guided-Wave Optics and the Corning's 2005 Stookey Award. He was a member of teams who won the 1999 Research and Development 100 Award for LEAF®fiber, the 2008 Research and Development 100 Award for ClearCurve®fiber, the 2008 ACS Northeast Regional Industrial Innovation Award, the Corning's 2016 Outstanding External Publication Award, and the 2017 ACS Heroes of Chemistry Award. He has served as an Associate Editor, a Coordinating Committee Member, and the Deputy Editor for the *Journal of Lightwave Technology*. He has also served as a guest editor for several special issues and as committee chair or member for many international conferences.

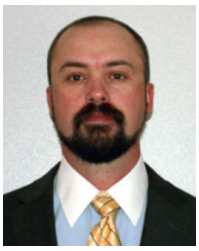

JOSHUA DAW received the Ph.D. degree in mechanical engineering from the University of Idaho.

He is currently a Research Scientist and an Engineer with the INL's High Temperature Test Laboratory, where he developed instrumentation for in-core irradiation tests. He also leads development and deployment efforts for in-core ultrasonic instrumentation. He has authored or coauthored 12 peer reviewed journal publications and 21 peer-reviewed conference papers on high temperature testing and in-pile instrumentation. As a University of Idaho graduate student, he received several recognition awards for his research on high-temperature in-core instrumentation. He was awarded the 2013 Laboratory Director's Award for exceptional engineering achievement.

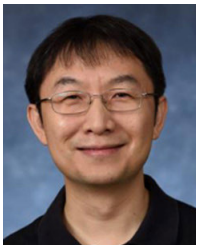

ZHI-HONG MAO (Senior Member, IEEE) received the dual bachelor's degree in automatic control and applied mathematics from Tsinghua University, Beijing, China, in 1995, and the Ph.D. degree in medical engineering and medical physics from the Harvard–MIT Division of Health Sciences and Technology, Cambridge, MA, USA, in 2006. He joined the University of Pittsburgh, Pittsburgh, PA, USA, as an Assistant Professor, in 2005, and became a Professor, in 2018.

CYRIL HNATOVSKY received the M.Sc. degree in physics from the University of Toronto, Toronto, ON, Canada, in 1999, and the Ph.D. degree in physics from the University of Ottawa, Ottawa, ON, Canada, in 2006.

He is currently a Research Officer with the National Research Council Canada working on different projects related to the inscription of Bragg gratings in optical fibers. His research interests mainly include the interaction of sub-picosecond laser pulses with solids, including the development of advanced material processing methodologies and their application for prototyping of photonic and microfluidic devices.

STEPHEN J. MIHAILOV (Senior Member, IEEE) received the B.Sc. degree in physics from Carleton University, Ottawa, Canada, in 1986, and the Ph.D. degree in physics from York University, Toronto, Canada, in 1992. He studied excimer laser processing of polymers with York University.

He currently leads the Fiber Photonics Group within the Security and Disruptive Technologies Research Centre of the National Research Council Canada (SDT-NRC). He is recognized internationally as an expert in fiber optics and FBG technology. He has coauthored over 260 peer-reviewed international book, and journal and conference publications. He is a co-inventor of 21 issued U.S. patents. He is a fellow of the Optical Society of America (OSA)

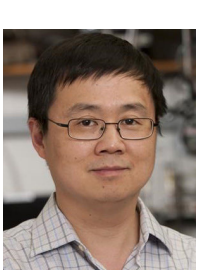

KEVIN P. CHEN received the Ph.D. degree in electrical engineering from the University of Toronto, Toronto, ON, Canada, in 2002. He joined the University of Pittsburgh, PA, USA, in 2002, after his Ph.D. training. He is currently a Paul E. Lego Chair Professor with the Department of Electrical and Computer Engineering, University of Pittsburgh. He has authored or coauthored over 300 scientific publications and over one dozen patents. His current research interests include fiber optics, integrated optics, laser processing, and laser spectroscopy.